arXiv:0806.4898v1 [cond-mat.mes-hall] 30 Jun 2008

BOUND STATES IN THE CONTINUUM IN TWO-DIMENSIONAL SERIAL STRUCTURES

Giorgio Cattapan

Dipartimento di Fisica "G. Galilei", Università di Padova,

Via F. Marzolo 8, I-35131 Padova, Italy

Istituto Nazionale di Fisica Nucleare, Sezione di Padova,

Via F. Marzolo 8, I-35131 Padova, Italy

Paolo Lotti*

Istituto Nazionale di Fisica Nucleare, Sezione di Padova,

Via F. Marzolo 8, I-35131 Padova, Italy

Abstract

We investigate the occurrence of bound states in the continuum (BIC's) in serial structures of quantum dots coupled to an external waveguide, when some characteristic length of the system is changed. By resorting to a multichannel scattering-matrix approach, we show that BIC's do actually occur in two–dimensional serial structures, and that they are a robust effect. When a BIC is produced in a two–dot system, it also occurs for several coupled dots. We also show that the complex dependence of the conductance upon the geometry of the device allows for a simple picture in terms of the resonance pole motion in the multi–sheeted Riemann energy surface. Finally, we show that in correspondence to a zero–width state for the open system one has a multiplet of degenerate eigenenergies for the associated closed serial system, thereby generalizing results previously obtained for single dots and two-dot devices.

PACS numbers: 73.63.Nm Quantum wires, 73.23.Ad Ballistic transport, 73.21.La Quantum dots, 73.21.Cd Superlattices

*I would like to acknowledge the Physics Department of Padua University for hospitality and support.

I. INTRODUCTION

Since the seminal paper by von Neumann and Wigner [1], the occurrence of isolated discrete eigenvalues embedded in the continuum of scattering states has been the subject of several studies. Bound states in the continuum (BIC's) have been found by Fonda and Newton for a model two-channel system with square well potentials [2], and by Friedrich and Wintgen for the hydrogen atom in a uniform magnetic field [3]. More generally, resorting to Feshbach's theory of resonances, Friedrich and Wintgen were able to prove that BIC's can occur because of the interference of resonances belonging to different channels [4]. When the relative position of the resonances changes as a function of a continuous parameter of the system, their interference produces an avoided crossing of the resonance positions; at the same time, a dramatic change in their widths occurs, and for a given value of the parameter one of the resonances acquires an exactly vanishing width, thereby becoming a BIC.

More recently, the existence of BIC's have been proved for quantum dots coupled to reservoirs. Zero-width states have been found in serial structures of dots or loops within simple, one-dimensional models of mesoscopic systems [5]. That BIC's are a general phenomenon of quantum dots has been shown by Sadreev *et al.*, by modeling a quantum dot as a single billiard of variable shape attached to an external lead [6]. By resorting to an effective Hamiltonian approach to electron scattering through the device [7, 8], the resonance features of the transmission probability have been related to the spectral properties of the closed quantum billiard. In particular, it has been found that zero-width states appear in the continuum of the open system, near the points of degeneracy or quasi-degeneracy of the closed-system eigenenergies. Two-dot systems have been studied as well, either through analytically soluble models allowing for a small number of discrete states in each dot [9], or through direct numerical solution of the two-dimensional Schrödinger equation via the contour integration method [10]. In the former case, BIC's appear again when the eigenenergies of the closed system cross the transmission zeros, with the electrons being trapped within the device [9]. In ref. [10], zero-width resonances have been analyzed in terms of the motion of the corresponding S-matrix poles in the complex energy plane. In analogy to what has been found for the usual coupled–channel problem [3, 4], the onset of zero–width states is associated to couples of poles, moving counterclockwise in the energy plane as the bridge length increases, one of the poles touching the real energy axis at critical values of

this parameter. Moreover, BIC's appear at nearly periodic distances between the dots, when the length of the connecting bridge is varied.

The aim of the present paper is to extend the analysis of resonances, and of their evolution into BIC's as some continuous parameter of the system varies, to *two-dimensional* serial structures of dots. As is well–known, when several identical elements, such as dots, rings or constrictions, are connected in series, a band structure emerges in the transmission coefficient. In the same way as a band structure for electrons appears in solid–state physics [11, 12], one has alternating regions of allowed and of essentially zero transmission as a function of energy. A noteworthy feature of periodic mesoscopic systems is that this "miniband" structure appears even for a relatively small number $(3 \div 5)$ of components [11]. We numerically solve the two–dimensional Schrödinger equation by a combination of mode–matching and S-matrix techniques, the total scattering operator for the device being obtained from the S–matrices referring to the various segments of the system through the $\star$–product composition rule [13, 14, 15]. This approach provides numerically stable results for both physical and complex values of the energy, even when some dimension of the system is large [15], and has been already employed by us to investigate Fano resonances and threshold phenomena in ballistic transmission through dots with impurities [15, 16]. In studying zero–width states in serial systems, three issues will be of particular concern to us; *i*) how robust these trapped states are when the number of segments increases; in other words, given the occurrence of a BIC in, say, a two–dot system for a given configuration, there is a similar state for the analogous several-dots device?; *ii*) whether and to what extent the close relationship among zero–width states and the eigenstates of the *closed* system found for a single dot (or a coupled–dot pair) extends to serial structures; *iii*) what happens when the translational symmetry of the system is broken in correspondence to a BIC configuration by varying the dimensions of the central dot.

The paper is organized as follows. In Section II we recall the main characteristics of our approach, and present the results for serial systems of dots coupled to a common waveguide. The non–trivial changes of the transmission coefficients as some parameter of the device is varied will be given a simple, transparent interpretation in the light of the motion of the resonance poles in the complex energy plane. Our main conclusions will be summarized in Section III.

II. ZERO-WIDTH STATES IN MULTI-MODE SERIAL STRUCTURES

We shall consider the device illustrated in Figure 1. The quantum dots are modeled as rectangular cavities of total width c and length l_d, connected through bridges of width b and length l_b. The whole system is coupled to a uniform guide of indefinite length, having the same width as the connecting necks. In the ballistic regime, the electronic transport through the device can be described as a scattering process, and the conductivity of the quantum circuit can be expressed in terms of the transmission coefficients of the system [13, 14]. To evaluate these quantities, we start from the two–dimensional Schrödinger equation

$$\left\{ -\frac{\hbar^2}{2m^*} \nabla_2^2 \right\} \Psi(x,y) = E\Psi(x,y) \quad , \tag{2.1}$$

where ∇_2^2 represents the two–dimensional Laplace operator, E is the total energy, and m^* is the electron's effective mass in the conduction band. Eq. 2.1 has been solved by a suitable

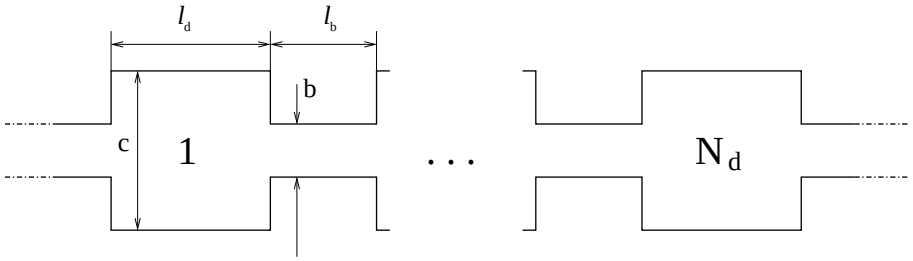

FIG. 1: A serial structure of N_d quantum dots coupled to an infinite external lead.

combination of mode–matching and S–matrix techniques, as detailed in Refs. [15, 16], to which we refer the reader for details. Expanding the total wave–function into complete sets of transverse–mode eigenfunctions in the various segments (dots and bridges) of the device, Eq. 2.1 is reduced to a set of one–dimensional Schrödinger equations for the expansion coefficients, which depend upon the propagation variable x only. These coefficients are written in terms of forward and backward propagating waves, with amplitudes which can be related to one another matching the wave function and its first derivative at the various interfaces delimiting the necks from the dots and the whole device from the external ducts. The scattering operator for each segment is given once the amplitudes of the waves leaving an interface are expressed linearly in terms of the coefficients of the incoming waves. The

total S–matrix

$$\mathbf{S} = \begin{pmatrix} \mathbf{S}_{11} & \mathbf{S}_{12} \\ \mathbf{S}_{21} & \mathbf{S}_{22} \end{pmatrix} \tag{2.2}$$

is finally obtained from the partial scattering operators through a recursive application of the $\star$–product composition rule [13, 15]. In so doing, a different number of modes can be introduced in the various segments of the device, to improve convergence, and evanescent modes can be taken into account while preserving the numerical accuracy of the calculation, even when some dimension of the system gets large. The transmission coefficients are contained in the matrix blocks $\mathbf{S}_{12}$ and $\mathbf{S}_{21}$; more precisely, $(\mathbf{S}_{21})_{nm}$ represents the transmission coefficient to mode n on the right of the device for an electron impinging from the left in mode m, whereas $(\mathbf{S}_{12})_{nm}$ is the transmission coefficient to the final mode n on the left from the initial mode m on the right. The sub-matrices $\mathbf{S}_{11}$ and $\mathbf{S}_{22}$ contain, on the other hand, the corresponding reflection coefficients to the left and to the right.

The scattering problem has been solved for an electron impinging from the left, with outgoing reflected and transmitted waves in all the open channels, and the total conductance G (in units $2e^2/h$) has been evaluated through the two–probe Büttiker formula [13, 14]

$$G = \sum_{m,n} \frac{k_n^{(l)}}{k_m^{(l)}} \left| (\mathbf{S}_{21})_{nm} \right|^2 \quad , \tag{2.3}$$

where the sum is restricted to the open channels only, and the propagation wave numbers $k_n^{(l)}$ in the external leads are related to the total energy E by [15]

$$k_n^{(l)} \equiv \sqrt{\frac{2m^*}{\hbar^2} E - \left(\frac{n\pi}{b}\right)^2} \quad .$$

As in our previous papers [15, 16], convergence is fully achieved when four channels are included in the leads, and up to 10 channels are taken into account in the dots; fairly good results are already obtained, however, with 2 and 5 modes in the lead and in the dots, respectively. For the evanescent modes, the propagation wave-numbers are taken as purely imaginary quantities, with a positive coefficient, namely $k_n^{(l)} = i\sqrt{(n\pi/b)^2 - 2m^*E/\hbar^2}$.

In figure 2 we plot the conductance as a function of the energy for various serial devices, with an increasing number N_d of dots. For the sake of simplicity, we have limited ourselves to the first subband, where only one propagating mode is active. To have the results independent from the actual size of the device, we measured all lengths in terms

of the waveguide width b, and energies with respect to the waveguide fundamental mode $\epsilon_1^{(l)} \equiv \frac{\hbar^2}{2m^*}\left(\frac{\pi}{b}\right)^2$. Adimensional quantities will be denoted with the "tilde" symbol, so that the various thresholds $\epsilon_n^{(l)} = n^2\epsilon_1^{(l)}$ are simply given by $\tilde{\epsilon}_n^{(l)} = n^2$, with $n = 1, 2, 3, \ldots$. The calculations reported in Figure 2 refer to devices with a bridge length $\tilde{l}_b \equiv l_b/b = 3.9$. The dots are modeled by square cavities with $\tilde{c} = \tilde{l}_d = 2$, symmetrically coupled to the bridges as well as to the waveguide.

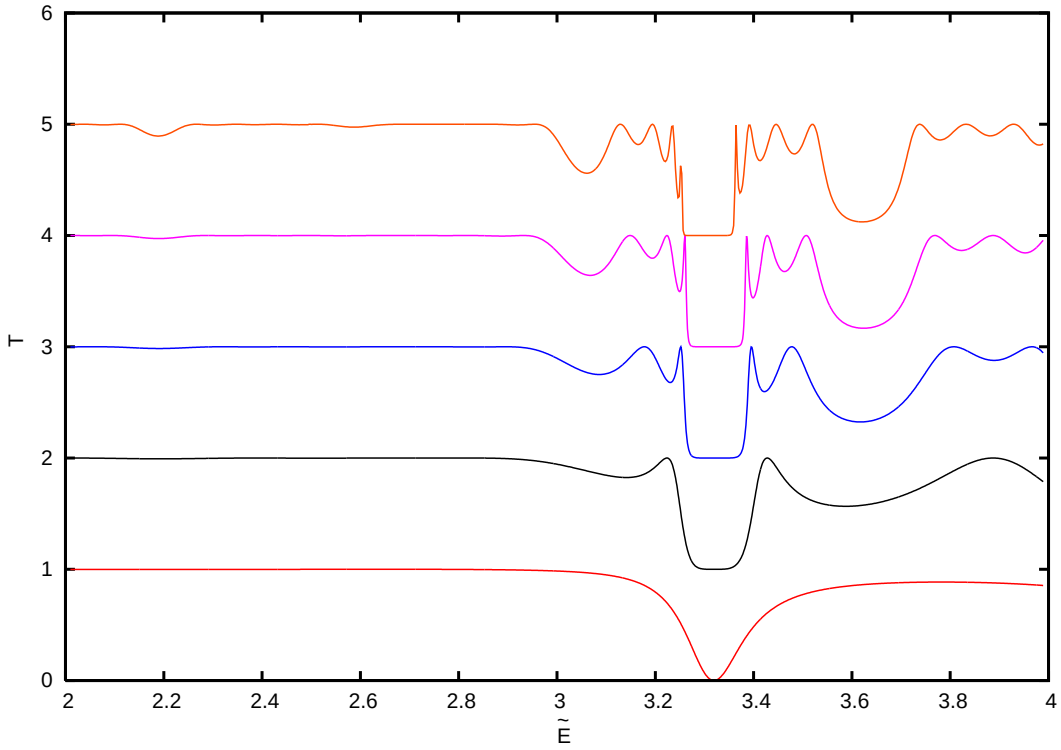

FIG. 2: Total transmission as a function of the adimensional energy for increasing number of dots. From bottom to top $N_d = 1, 2, 3, 4, 5$. Consecutive curves are vertically offset for clarity.

As N_d increases from 2 to 5, one sees $1, 2, 3, 4$ peaks on each side of the transmission zero at $\tilde{E} \sim 3.3$. One moreover observes a more and more structured conductance profile at the upper edge of the band, and a smooth plateau of maximum transmission in the low–energy part of the considered energy region. The most interesting feature of Figure 2 is the multiplet of peaks around the transmission zero at $\tilde{E} \sim 3.3$, having a position almost independent upon the number of coupled dots. The increase in the number of oscillations is due to the more and more complex interference pattern among the waves reflected and transmitted at the dots, and has been previously found both in one–dimensional serial structures [5, 17, 18], and in periodic, two-dimensional waveguides with stubs and constrictions [19, 20, 21].

In figure 3 we plot (from bottom to top) the conductance of a 5-dot device in the first energy subband, for $\tilde{l}_b$ increasing from 3.3 up to 3.9, in steps of 0.1. As $\tilde{l}_b$ gets longer, the resonance peaks move towards lower energies, the typical binding effect one observes when some characteristic length of the system increases [15]. At the same time, the four peaks on the right of the transmission zero (numbered from 1 to 4 in figure 3) approach each other and the transmission minimum, until they disappear for $\tilde{l}_b = 3.6$, where a zero-width state is produced. For longer bridge lengths, they appear again on the left of the transmission minimum, with increasing relative distances. The four peaks on the left of the transmission zero for $\tilde{l}_b = 3.3$, on the other hand, have in the mean time merged into the low energy background discernible in figure 3. One observes also peaks moving down in energy, coming from the second scattering threshold, at $\tilde{E} = 4$. For $\tilde{l}_b = 3.9$ a conductance profile quite similar to the initial one can be observed. The same trend is observed for a different number of dots, with the BIC occurring more or less at the same energy position and almost for the same value of the bridge length.

As Figure 3 exhibits, the behavior of the conductance as a function of energy with varying bridge length is by far non trivial. A simpler picture emerges, when one considers the motion of the S–matrix poles in the multi–sheeted energy Riemann surface. For the present purposes, one can limit oneself to the Riemann sheet where $\mathrm{Im}k_1^{(l)} < 0$ whereas $\mathrm{Im}k_j^{(l)} > 0$ for $j > 1$; there, one has exponentially diverging waves in the open channel, and exponentially decreasing waves in the other channels. A pole at $E_p \equiv E^{(R)} - i\Gamma$ can be associated to a resonance in the conductance G around $E \sim E^{(R)}$, of width 2Γ, provided that $E^{(R)}$ is in between the first and second scattering threshold [16, 22]. We applied our approach to solve the Schrödinger equation for complex energies and channel momenta, so as to locate the S–matrix poles in the relevant sheet. The results are given in Figures 4 and 5. In the lower panel of the former we give the four poles corresponding to peaks $1 \div 4$ in figure 3, while in the latter we plot the poles associated to peaks $5 \div 8$. As $\tilde{l}_b$ increases from $\tilde{l}_b = 3.3$ up to $\tilde{l}_b = 3.6$, the poles of figure 4 rotate counterclockwise in the fourth quadrant of the energy plane approaching the real energy axis, where they collapse and coincide with the transmission zero for $\tilde{l}_b = 3.6$. As the bridge length increases further, the four poles move away from the energy axis, so that the corresponding peaks are again discernible in the conductance at lower and lower energies. As for the poles at the upper edge of the transmission band, they move monotonically downwards in the energy plane towards the

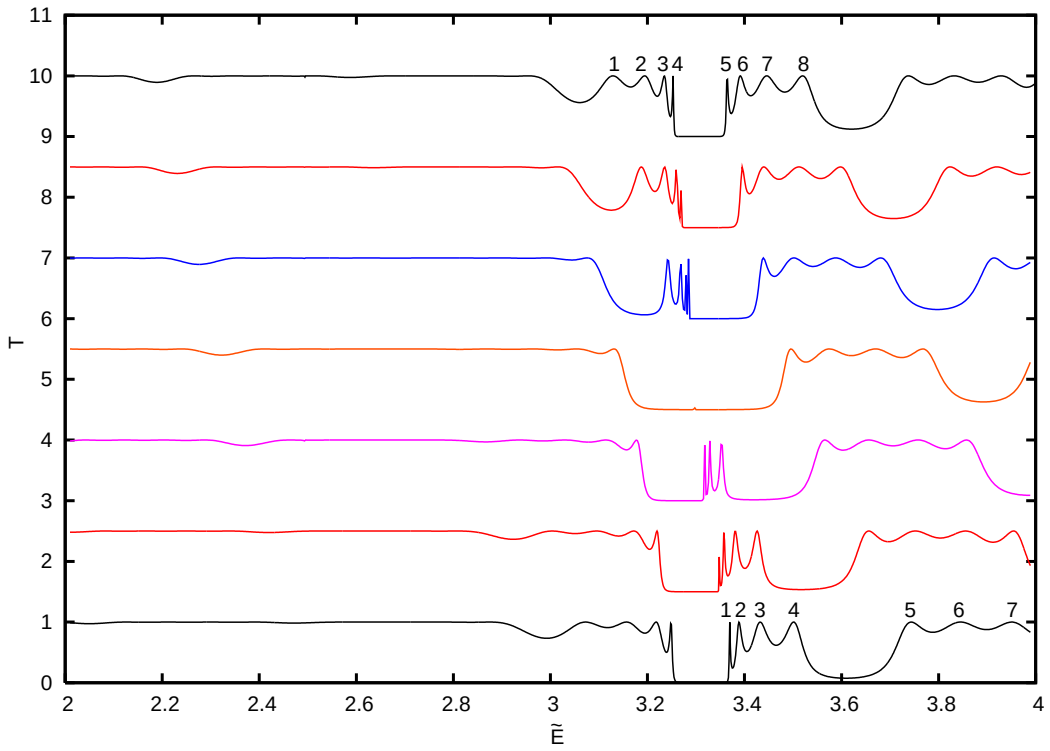

FIG. 3: Total conductance of 5 square dots symmetrically coupled to a waveguide as a function of the adimensional energy. Each dot has $\tilde{c} = \tilde{l}_d = 2.0$. From bottom to top the bridge length $\tilde{l}_b$ increases from $\tilde{l}_b = 3.3$ up to $\tilde{l}_b = 3.9$ with $\Delta\tilde{l}_b = 0.1$. The numbers $1, \ldots, 8$ label the peaks to which we refer in the text. Consecutive curves are vertically offset for clarity.

energy axis until they produce peaks $5 \div 8$ at the right of the transmission minimum, which can be seen in figure 3 for $\tilde{l}_b = 3.9$. In the mean time, new poles come into play through the second scattering threshold, coming from the higher energy region. As far as these poles have $E^{(R)} > 4$, however, they cannot produce observable effects on the conductance; indeed, transmission resonances above the second scattering threshold are due to poles residing on other, different sheets of the energy Riemann surface [16]. Stated in the language of dispersion theory, as the bridge length increases one observes that some of the S–matrix poles undergo a transition from a "shadow" state to a "dominant" role [16, 23]. We verified also that the low energy plateau in the conductance corresponds to a group of closed packed poles in the energy plane. As $\tilde{l}_b$ increases, the four poles producing the peaks on the left of the transmission zero for $\tilde{l}_b = 3.3$ join these low energy poles so that the corresponding peaks disappear in the background.

For greater bridge lengths a zero–width state appears again at $\tilde{E} \sim 3.3$ in the conductance

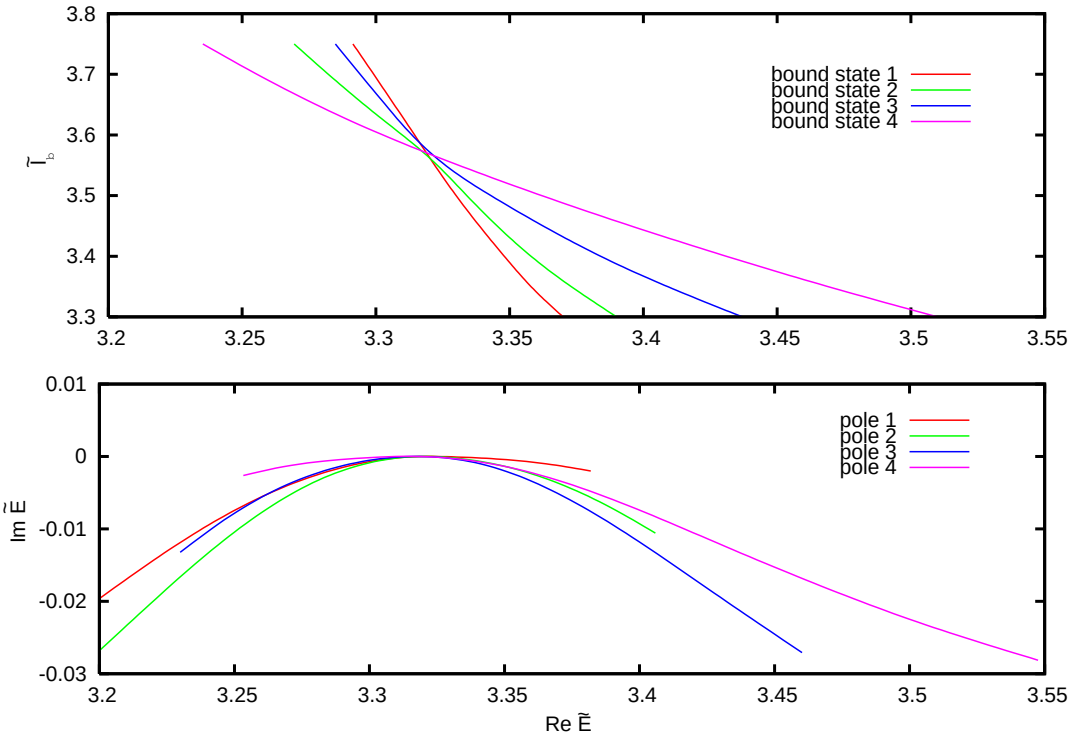

FIG. 4: Lower panel: counterclockwise motion of the poles associated to the peaks $1, 2, 3, 4$ of Figure 3 in the complex energy plane for $\tilde{l}_b$ increasing from 3.3 up to 3.9. Upper panel: the associated eigenenergies of the corresponding closed system in the $(\tilde{E},\ \tilde{l}_b)$ plane.

spectrum. This is exhibited in the left-most part of Figure 5, where we give also the pole positions for $\tilde{l}_b \geq 3.9$; for $\tilde{l}_b = 4.22$ the four poles coincide with each other and with the transmission zero, and a new BIC appears. Note that the four poles associated to the BIC at $\tilde{l}_b = 3.3$ have in the meantime moved downward in energy towards the structureless background. It is finally worth to mention what happens in terms of the S–matrix poles when the number of dots increases for a given bridge length. With reference to Figure 1, the dip in conductance one observes for $N_d = 1$ is due to a pole at $E_p \simeq 3.31 - 0.072i$; no other pole is found near the energy axis in the considered energy region. Things are already quite different when passing to the two–dot case; the smooth plateau of maximum transmission at low–energy is associated to four closed–packed poles with $2.03 < E^{(R)} < 3.02$ and $0.303 < \Gamma < 0.379$. As N_d increases, more and more strongly coupled poles appear in the low-energy part of the first transmission band. At the same time, more and more poles appear very near the energy axis, on both sides of the transmission zero. In all instances, the transmission zero occurs at $\tilde{E} \simeq 3.32$.

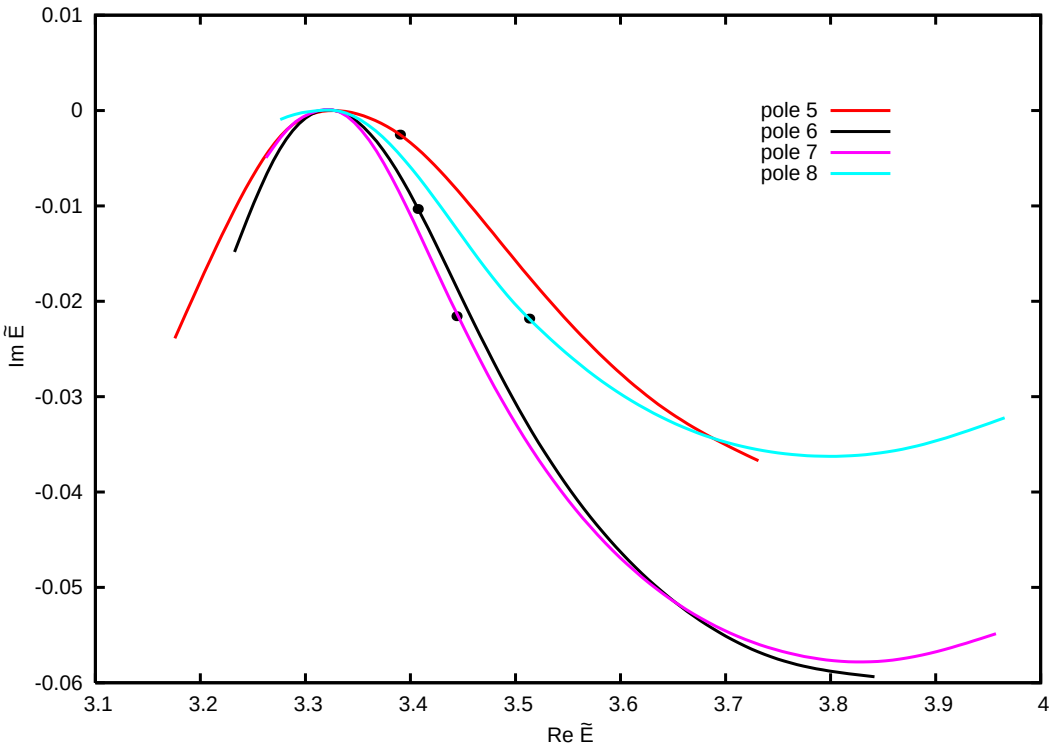

FIG. 5: Counterclockwise motion of the poles $5, 6, 7, 8$ of Figure 3 in the complex energy plane with l_b increasing from $\tilde{l}_b = 3.3$ up to $\tilde{l}_b = 4.5$. The full dots mark the pole positions for $\tilde{l}_b = 3.9$.

For coupled–channel problems in Atomic Physics, the dynamics underlying the occurrence of BIC's has been investigated by Friedrich and Wintgen in the framework of a three–channel model [3, 4]. Assuming one open and two closed channels, where the wave function is taken to be proportional to the bound-state solutions of the corresponding uncoupled Schrödinger equations, one can solve for the scattering component so as to obtain explicit expressions for the resonance positions and widths. Friedrich and Wintgen were able to show that, as the bound state energies E_1 and E_2 were tuned varying some characteristic parameter, the interference effects lead to an avoided crossing of the resonance positions. At the same time, one observes dramatic changes in the resonance widths, one of them vanishing when $E_1 = E_2$ and the bound states in the uncoupled closed channels become degenerate. A strict connection between the occurrence of zero-width resonances and the presence of degenerate eigenenergies for the corresponding *two-dimensional closed* system has been also found for a quantum billiard of variable shape by Sadreev *et al.* [6]. The two-dot case has been considered in Ref. [9]. There too, the trapping of the particle in the internal bridge occurs in correspondence to the crossing of the transmission zero by the eigenenergies of the closed

system. We ascertained whether this simple relation between the occurrence of zero–width states and the eigenenergies of the closed system still holds in the serial structures under consideration. To this end, one has to solve the Dirichlet boundary–value problem for periodic domains such that of Figure 1. We accomplished this through a modification of the S–matrix approach. The condition that the full wave–function vanishes on the leftmost and rightmost edge of the closed system implies that the amplitudes of the forward and backward propagating waves have to be related by

$$\overrightarrow{c}_n^{(1)} = -\overleftarrow{c}_n^{(1)} \quad \overrightarrow{c}_n^{(N_d)} = -e^{-2i\tilde{k}_n^{(d)}\tilde{l}_d}\overleftarrow{c}_n^{(N_d)} \quad , \tag{2.4}$$

where $\overrightarrow{c}_n^{(1)}$ and $\overleftarrow{c}_n^{(1)}$ are the amplitudes for the waves propagating in the first dot to the right and to the left, respectively, and $\overrightarrow{c}_n^{(N_d)}$, $\overleftarrow{c}_n^{(N_d)}$ the corresponding quantities in the last dot on the right. By $\tilde{k}_n^{(d)}$ we denote the adimensional propagation wave numbers in the various channels inside the dots [15]. Note that, even if these relations have been written for an open channel, they apply in the closed channels also, so that convergence with respect to the expansion into transverse basis functions is guaranteed when solving the Dirichlet problem in the domain. Now, by definition of the S–matrix, one can write in obvious matrix notation

$$\begin{pmatrix} \overleftarrow{\mathbf{c}}^{(1)} \\ \\ \overrightarrow{\mathbf{c}}^{(N_d)} \end{pmatrix} = \begin{pmatrix} \mathbf{S}_{11} & \mathbf{S}_{12} \\ \\ \mathbf{S}_{21} & \mathbf{S}_{22} \end{pmatrix} \begin{pmatrix} \overrightarrow{\mathbf{c}}^{(1)} \\ \\ \overleftarrow{\mathbf{c}}^{(N_d)} \end{pmatrix} \quad . \tag{2.5}$$

Combining Eqs. 2.4 and 2.5 one obtains

$$\mathcal{B}\overrightarrow{\mathbf{c}}^{(N_d)} = 0 \quad , \tag{2.6}$$

where

$$\mathcal{B} \equiv \mathbf{S}_{21}\left(\mathbf{1} + \mathbf{S}_{11}\right)^{-1}\mathbf{S}_{12}\mathbf{\Omega} - \mathbf{S}_{22}\mathbf{\Omega} - \mathbf{1} \quad , \tag{2.7}$$

with $\mathbf{\Omega}_{mn} \equiv e^{2i\tilde{k}_m^{(d)}\tilde{l}_d}\delta_{mn}$. Eq. 2.6 represents a system of homogeneous equations for the amplitudes $\overrightarrow{c}_n^{(N_d)}$, which has a non–trivial solution if and only if the condition $\det\mathcal{B} = 0$ is satisfied. This condition can be regarded as the secular equation fixing the eigenenergies of the standing waves in the closed, periodic domain under consideration. Since the energy enters in a highly non–trivial way in the secular equation through the channel wave-numbers, we actually evaluated $\det\mathcal{B}$ for varying energies, and looked for the zeros of its modulus through a minimization procedure. We tested our approach for a rectangular domain, whose eigenenergies are known analytically, and for the quarter square Sinai billiard, which has

been studied by different means in Ref. [24]. We found excellent agreement in both cases when the same number of basis functions as in the scattering calculations were included.

In the upper panel of Figure 4 we exhibit the results of our calculations for the 5-stub case. The eigenenergies are plotted in the $(\tilde{E}, \tilde{l}_b)$ plane, and refer to the states associated with peaks $1 \div 4$, occurring when the system is coupled to the waveguide. From a comparison with the motion of the corresponding S-matrix poles (lower panel) one sees that, as the resonance poles move towards the energy axis and overlap the transmission zero in correspondence to the BIC, the eigenenergies of the closed system become closer and closer to each other, until one has four degenerate eigenvalues for $\tilde{l}_b = 3.6$. We verified that for three or four coupled dots one has a pair or a triplet of degenerate eigenenergies of the closed structure in correspondence to the BIC. The zero-width configuration occurs moreover practically at the same value of $\tilde{l}_b$. Overall, our findings show that the occurrence of trapped states with zero width is a *robust effect* in serial structures.

We looked also for possible avoided crossings between the trajectories of the resonance poles. In Figure 6 we give the real part of the pole energies $\tilde{E}_p$ for the pairs of poles (1, 5) and (2, 6) in the $(\tilde{E}, \tilde{l}_b)$ plane. The avoided crossing is clearly discernible for the lowest-energy resonances, as can be inferred from the lower panel of Figure 6; for $\tilde{l}_b = 3.6$, where the width of one of the resonances is zero, the relative distance among the corresponding poles reaches a minimum, and then increases again. This behavior is less evident for the other resonance, as the upper panel of Figure 6 shows, and deteriorates further as one considers the resonance poles at higher energies. This effect can be attributed to the presence of other, nearby poles at the upper edge of the transmission band. In particular, as the bridge length increases, more poles come into play from higher energies through the second scattering threshold, and may perturb the motion of the high–lying resonance poles of the upper multiplet.

We finally investigated the effect of a symmetry breaking of the system on the BIC. To be definite, we refer again to the 5–dot case with $\tilde{l}_b = 3.6$. When the central dot is made different from the lateral ones, the quadruplet of poles at the transmission zero are no longer degenerate, nor they coincide with the transmission zero. This removal of the BIC when the symmetry among the various dots is slightly broken is consistent with the results of ref. [9] for the two-dot case. The general rule according to which there is an antibinding effect, and the poles move in a counterclockwise way as some characteristic length of the system increases, is still obeyed. The four poles, however, move in the complex energy plane

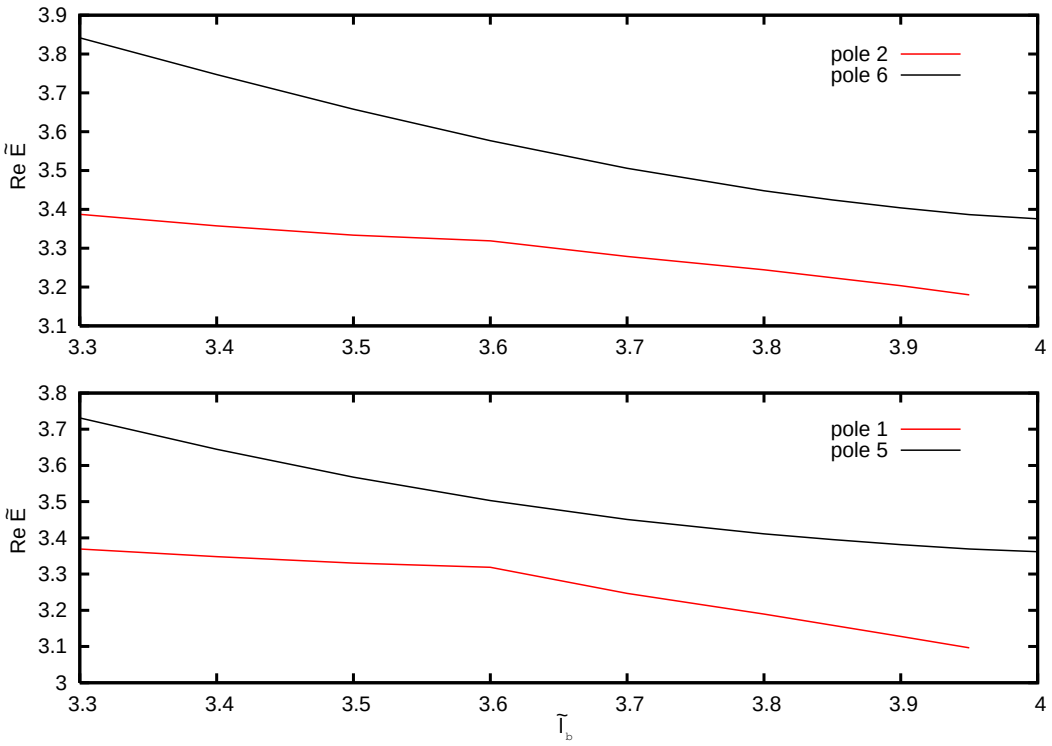

FIG. 6: Position of the resonances 1 and 5 as a function of $\tilde{l}_b$ for the 5-dot system of Figure 3 near the BIC configuration (lower panel). The same graph is given for resonances 2 and 6 in the upper panel.

with different velocities, producing a multiplet of narrow peaks which depend in a rather complex way upon the bridge length. In particular, when the central dot is made shorter with respect to the external ones, two poles move faster towards higher energies leaving the BIC position, until they give rise to peaks strongly coupled to the resonances residing at the upper edge of the conduction band. The other two poles of the quadruplet, on the contrary, do not leave the region of the transmission zero, and give rise to very narrow peaks in the limiting situation of a central dot of the same height as the connecting bridge, so that one has two couples of dots connected by a central bridge with $\tilde{l}_b = 9.2$.

III. CONCLUSIONS

In this paper we have considered the occurrence of zero–width states in the continuum of periodic systems of several coupled dots opened into an external waveguide. The present analysis can be therefore considered as the extension to serial devices of what has been

done for two–dot systems [9, 10]. We studied how the transmission properties change as the length $\tilde{l}_b$ of the connecting bridges varies, and found that the BIC phenomenon is a rather robust effect with respect to the number of dots N_d. When a BIC is produced for a suitable value of $\tilde{l}_b$ in a two–dot system, it persists for a larger number N_d of dots. Even if we limited ourselves to present detailed results for a 5–dot device, we verified that our conclusions still hold up to ten coupled dots. Overall, with varying $\tilde{l}_b$ the conductance profile varies in a non–trivial way. A much simpler picture emerges, however, when one looks at the trajectories of the resonance poles on the relevant sheet of the complex energy plane. As $\tilde{l}_b$ increases, the poles move counterclockwise in the energy plane; when a multiplet of poles collapses onto a transmission zero on the real energy axis the electron is trapped inside the device and a zero–width state emerges. This peculiar configuration is removed once the translational symmetry of the system is broken. Finally, we have shown that the present S–matrix approach can be modified so as to treat the Dirichlet boundary–value problem for the closed system. In close analogy with what has been found for a single [6], or two coupled dots [9], we found that in correspondence to a BIC a whole multiplet of eigenenergies of the closed system is degenerate with the transmission minimum.

---

[1] J. von Neumann, E. Wigner, Phys. Z. **30**, 465 (1929).

[2] L. Fonda, R. G. Newton, Ann. Phys. (N.Y.) **10**, 490 (1960).

[3] H. Friedrich, D. Wintgen, Phys. Rev. A **31**, 3964 (1985).

[4] H. Friedrich, D. Wintgen, Phys. Rev. A **32**, 3231 (1985).

[5] P. Singha Deo, A. M. Jayannavar, Phys. Rev. B **50**, 11629 (1994).

[6] A. F. Sadreev, E. N. Bulgakov, I. Rotter, Phys. Rev. B **73**, 235342 (2006).

[7] F. M. Dittes, Phys. Rep. **339**, 215 (2000).

[8] J. Okołowicz, M. Płoszajczak, I. Rotter, Phys. Rep. **374**, 271 (2003).

[9] A. F. Sadreev, E. N. Bulgakov, I. Rotter, J. Phys. A: Math. Gen. **38**, 10647 (2005).

[10] G. Ordonez, K. Na, S. Kim, Phys. Rev. A **73**, 022113 (2006).

[11] J. T. Londergan, J. P. Carini, D. P. Murdock, *Binding and scattering in two–dimensional systems* (Springer, Berlin, 1999).

[12] P. Pereyra, E. Castillo, Phys. Rev. B **65**, 205120 (2002).

[13] S. Datta, *Electronic Transport in Mesoscopic Systems* (Cambridge University Press, Cambridge, 1995).

[14] D. K. Ferry, S. M. Goodnick, *Transport in Nanostructures* (Cambridge University Press, Cambridge, 1997).

[15] G. Cattapan, P. Lotti, Eur. Phys. J. B **60**, 51 (2007).

[16] G. Cattapan, P. Lotti, Eur. Phys. J. B **60**,181 (2007).

[17] X.-W. Liu, A. P. Stamp, Phys. Rev. B **47**, 16605 (1993).

[18] Z. Y. Zeng, L. D. Zhang, X. H. Yan, J. Q. You, Phys. Rev. B **60**, 1515 (1999).

[19] K. Nikolić, R. Šordan, Phys. Rev. B **58**, 9631 (1998).

[20] Y. P. Chen, Y. E. Xie, X. H. Yan, Phys. Rev. B **74**, 035310 (2006).

[21] Y. P. Chen, Y. E. Xie, X. H. Yan, Phys. Rev. B **76**, 115439 (2007).

[22] A. M. Badalyan, L. P. Kok, M. I. Polikarpov, Yu. A. Simonov, Phys. Rep. **82**, 31 (1982).

[23] R.J. Eden, J.R. Taylor, Phys. Rev. B **133**, 1575 (1964).

[24] F.M. Zanetti, E. Vicentini, M.G.E. da Luz, Ann. Phys. (N.Y.) (2008) doi: 10.1016/j.a.op.2008.01.008, in press.